15 June 2001

ELSEVIER

Chemical Physics Letters 341 (2001) 107–114

CHEMICAL PHYSICS LETTERS

www.elsevier.nl/locate/cplett

Fast vibrational relaxation of OH($v = 9$) by ammonia and ozone

Sergey A. Nizkorodov, Warren W. Harper, David J. Nesbitt *

JILA, National Institute of Standards and Technology and University of Colorado, Boulder, CO 80309-0440, USA
JILA, Department of Chemistry and Biochemistry, University of Colorado, Boulder, CO 80309-0440, USA

Received 23 January 2001; in final form 27 February 2001

Abstract

Vibrational relaxation of OH($X^2\Pi$) in the $v = 9$ state by O_3 and NH_3 has been studied via flash-photolysis using high-resolution direct infrared absorption detection of OH in the $v = 11 \leftarrow 9$ band. OH($v = 9$) removal by O_3 occurs with a nearly gas-kinetic rate ($k_{O_3} = 1.37(15) \times 10^{-10}$ cm^3/s). Collisional removal by NH_3 ($k_{NH_3} = 7.60(50) \times 10^{-10}$ cm^3/s) is two to three times higher than the hard-sphere collision limit, suggesting a resonant V–V energy transfer induced by long-range dipole–dipole interactions. An upper limit of 5×10^{-14} cm^3/s is placed on OH($v = 9$) vibrational relaxation by argon.

1. Introduction

The hydroxyl radical (OH) plays an extremely important role in the chemistry of the Earth's atmosphere and other environments [1]. Though reaction and relaxation dynamics of OH are reasonably well understood in the troposphere and lower stratosphere, complete characterization in the higher atmospheric layers has remained elusive. A serious complication arises from the striking departure from local thermodynamic equilibrium [2] between molecular internal and translational degrees of freedom at these altitudes. As one dramatic example, intense emission from highly vibrationally ($v \leqslant 6$) and rotationally ($N \leqslant 33$) excited states of OH has been detected in the mesosphere [3]. Such results suggest more complicated dynamics for collisional quenching than previously appreciated, and further underscores the importance of quantitative kinetic studies of quantum-state specific relaxation rates for accurate modeling of atmospheric phenomena.

An ongoing effort in this laboratory is to investigate mechanisms responsible for populating these anomalously excited rotational states of OH (with $N \geqslant 30$ [3]) in the atmosphere. The main candidate reaction is $H + O_3$ [3]; however, it is not clear whether OH($N \geqslant 30$) is actually a direct albeit minor product of this reaction (believed to channel most of its exothermicity into the OH product vibrations [4,5]) or a result of secondary collision-induced vibration–rotation energy transfers. Our approach is to monitor the quantum-state resolved kinetics of OH(v, N) formation following pulsed UV photolysis of RH/O_3 mixtures ($RH = NH_3$, H_2, H_2S, etc.) by high-resolution direct absorption infrared spectroscopy. In the course of these studies, the vibrational relaxation

* Corresponding author. Fax: +1-303-492-5235.
E-mail address: djn@jila.colorado.edu (D.J. Nesbitt).

0009-2614/01/$ - see front matter
PII: S0009-2614(01)00371-2

of OH by NH_3 was found to be surprisingly rapid. Specifically, relaxation by ammonia occurs with a rate 2- to 3-fold higher than the gas-kinetic limit, which forms the main focus of this report. In this Letter we discuss the origin of this highly efficient relaxation and argue that it is consistent with a long-range dipole–dipole energy transfer mechanism.

2. Experimental

The experimental studies are conducted at $T = 295 \pm 2$ K in a 100 cm long, 5.1 cm diameter flow cell (Fig. 1) equipped with CaF_2 windows for good transmission at both UV photolysis (≈193 nm) and IR probe (≈2.7 μm) wavelengths. A collimated 8×8 mm^2 ArF-excimer laser beam operating at 5–10 Hz repetition rate propagates collinearly along the cell axis, with typical UV energies at the cell entrance of 1–5 mJ/pulse as continuously monitored at the cell exit using a calibrated thermopile. Real-time observation of OH($X^2\Pi$, $v = 9$) is accomplished using direct infrared absorption on the $v = 11 \leftarrow 9$ overtone band with a single mode ($\Delta\nu < 0.0001$ cm^{-1}) color center laser [6], which propagates collinearly down the flow cell and samples only the central 2–3 mm of the photolysis laser. Upon exiting the cell, the IR is separated from the excimer pulse with a dichroic mirror/grating combination and focused onto a liquid nitrogen cooled InSb detector. This study exploits high-resolution absorption on individual rovibrational, spin–orbit, and lambda doublet transitions in the $11 \leftarrow 9$ overtone band, which had not been investigated prior to this study. To facilitate this process, approximate frequencies for these $v = 11 \leftarrow 9$ transitions were estimated using OH term values from [7,8], which permitted the desired rovibrational transitions to be found with minimal spectral search (<1 cm^{-1}) and measured (<0.002 cm^{-1}) using standard wavemeter interferometry. The 24 OH($v = 11 \leftarrow 9$) transition frequencies utilized in this study are presented in Table 1.

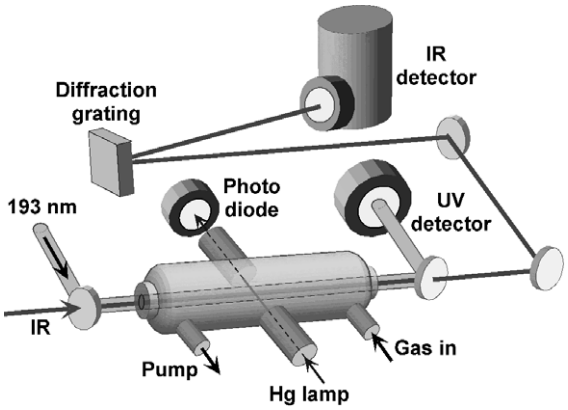

Fig. 1. Schematic diagram of the flash kinetic experimental apparatus. The density of O_3 is measured in situ using Hg-lamp absorption.

A portion of the IR radiation is split off before entering the cell and focused onto a reference detector. Balanced outputs from matched signal and reference detectors are electronically subtracted and averaged for 500–2000 UV laser pulses. Sets of

Table 1
Experimentally measured P-branch line positions (±0.01 cm^{-1} accuracy) for the previously unobserved $v = 11 \leftarrow 9$ band of OH[a]

J''	$P_{1e}(J'')$	$P_{1f}(J'')$	$P_{2e}(J'')$	$P_{2f}(J'')$
1.5			3855.04	3854.93
2.5	3838.45	3838.39	3823.58	3823.45
3.5	3808.23	3808.10	3788.69	3788.57
4.5	3774.75	3774.52	3750.50	3750.43
5.5	3737.99	3737.66	3709.12	3709.09
6.5	3697.95		3664.56	3664.60
7.5	3654.61			
8.5	3607.99			
9.5	3558.07			

[a] Where available, the measurements agree (±0.02 cm^{-1}) with predictions from term values for OH($v = 11$) and OH($v = 9$) reported in [7] and [8].

on- and off-resonance data are collected with the IR laser tuned on the OH absorption line as well as 5–10 Doppler widths away ($\Delta\nu_{Dop} \approx 300$ MHz). This compensates for weak broad band NH_2 chemiluminescence induced by UV photolysis (typically <10–20% of the OH peak absorbance), which is further suppressed with a diffraction grating in the probe beam path. The RMS noise in the final trace translates into an absorption sensitivity of $\leqslant 10^{-5}$ in a 1 MHz detection bandwidth, which, for a 300 K Doppler broadened peak, corresponds to an OH($v = 9$) detection sensitivity of $\leqslant 5 \times 10^8$ cm^{-3} per quantum state.

Commercial samples of ammonia (99.999%), argon (99.999%), and helium (99.9995%) are used without further purification. Ozone is produced from oxygen (99.99%) with a commercial ozonizer, trapped on silica gel beads at about 170 K, and introduced into the cell at a controlled flow rate with the trap warmed to 200–230 K. Argon (or helium) buffer gas and 2% NH_3/Ar mixture are injected into the cell through two calibrated flow controllers. Partial pressures of each gas in the mixture are obtained from flow rates and total cell pressure, as measured with calibrated 1 and 10 Torr capacitance gauges (1 Torr = 133.32 Pa). [O_3] is also probed directly in the flow cell using filtered Hg lamp absorption at 253.65 nm ($\sigma_{O_3} = 1.136 \times 10^{-17}$ cm^2 [9]), which permits in situ assessment of ozone purity (>90%) by comparison of flow and optical measurements. Absolute NH_3 concentrations are also verified from Beer's law absorption at the excimer wavelength, which agree with the more precise flow rate measurements within experimental uncertainty. Typical reagent and buffer-gas densities are 0–20 mTorr NH_3, 0–30 mTorr O_3, 1–7 Torr Ar (or He) for a 70–150 sccm total flow rate. A greater than 100-fold excess of buffer gas is present to ensure complete rotational/translational thermalization on a time-scale fast with respect to formation and loss rates in the OH($v = 9$) manifold.

3. Results

Fig. 2 displays typical time-resolved OH absorption traces with varying [NH_3] and [O_3] in the flow cell. Following the excimer laser pulse, the OH ($v = 11 \leftarrow 9$) absorption signal rises on a fast (≈5–15 μs) time-scale and then decays back to 0 on a much slower time-scale (≈50–200 μs). Production of OH($v = 9$) arises exclusively by reaction of H with O_3 (see below). Since this process cannot energetically populate the $v = 11$ state [4,5], the absorption signals directly probe the time-resolved density of OH($v = 9$). As in any pseudo first-order kinetic system, there is a potential ambiguity in whether the initial rise or subsequent decay corresponds to production or removal of the probed species. However, the OH($v = 9$) decay rate is observed to be independent of the NH_3 density but increases linearly with [O_3]. This confirms that the

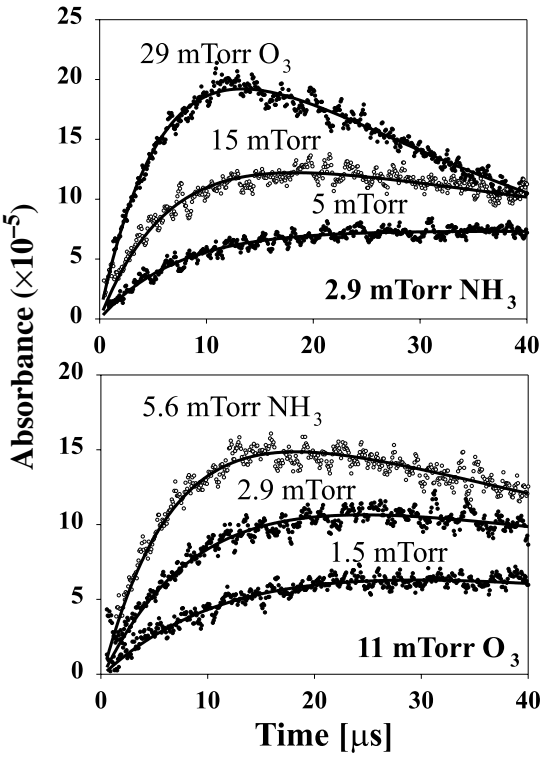

Fig. 2. Sample OH($v = 11 \leftarrow 9$) absorbance traces for various O_3 and NH_3 partial pressures monitored on the P_{1e} (3.5) transition at 3808.23 cm^{-1}. Higher [NH_3] or [O_3] produces shorter rise-times and larger peak signals, whereas the decay-time depends only on [O_3]. This confirms that the initial exponential *rise* is due to *removal* of OH($v = 9$) by O_3 and NH_3, and the long-time *decay* to *formation* of OH($v = 9$) by reaction of H with O_3.

slow *decay* corresponds to *formation* of OH(v) from $H + O_3$. In addition, the appearance rates (i.e., $1/\tau_{rise}$) increase linearly with both $[NH_3]$ and $[O_3]$, up to the detector limit ($\tau_{rise} < 1$ μs) at $[NH_3] \geqslant 1.5 \times 10^{15}$ cm^{-3} or $[O_3] \geqslant 6 \times 10^{15}$ cm^{-3}, which further supports the scenario that the fast *rise* is associated with *removal* of OH($v = 9$). Finally, the maximum OH absorbance signal intensities increase with both $[NH_3]$ and $[O_3]$; however this increase eventually saturates for either reactant in excess, again indicating a rise-time dominated by removal rather than production kinetics.

These observations are consistent with the following simple kinetic model for production and removal of OH($v = 9$)

$$NH_3 + 193\ \text{nm} \rightarrow H + NH_2, \tag{1}$$

$$H + O_3 \rightarrow OH(v = 6\text{–}9; N) + O_2, \tag{2}$$

where high-collision rates with excess buffer gas suffice to maintain the system in rotational equilibrium. This production rate is in competition with much faster vibrational and/or chemical removal of OH($v = 9$) by O_3, NH_3, or, possibly, by buffer gas M:

$$OH(v = 9) + O_3 \rightarrow \text{products}, \tag{3}$$

$$OH(v = 9) + NH_3 \rightarrow \text{products}, \tag{4}$$

$$OH(v = 9) + M \rightarrow OH(v < 9) + M. \tag{5}$$

If one assumes photolysis and rotational equilibration rates to be much faster than (2)–(5), the OH($v = 9$) time dependence can be solved analytically to yield

$$[OH(v = 9)] = \frac{k_{decay}[H]_0}{k_{rise} - k_{decay}} \left\{ e^{-k_{decay}t} - e^{-k_{rise}t} \right\},$$
$$k_{rise} = k_{O_3}[O_3] + k_{NH_3}[NH_3] + k_M[M], \tag{6}$$
$$k_{decay} = k_2[O_3],$$

where k_{O_3}, k_{NH_3}, and k_M are the corresponding bimolecular removal rates and the k_{rise} and k_{decay} are associated with the removal (3)–(5) and formation (2) processes, respectively. Note that the initial concentration of H atoms, $[H]_0$, is linearly proportional to $[NH_3]$.

The set of kinetic traces as a function of $[O_3]$ and $[NH_3]$ can be readily fit with least squares methods to a sum of single exponential rise and decay terms. From analysis of decay-times as a function of $[O_3]$, we obtain $k_2 = 2.4(2) \times 10^{-11}$ cm^3/s, which is in excellent agreement with the range of previously reported literature values, $2\text{–}3 \times 10^{-11}$ cm^3/s [10]. The analysis of rise-times is more involved since these can depend on densities of NH_3, O_3, and buffer gas (He or Ar). However, within experimental precision, the rise-times are independent of buffer-gas densities up to the highest pressures investigated (≈6.5 Torr). This indicates rapid rotational equilibration but negligible vibrational relaxation on the <100 μs time-scale, which places a conservative upper limit of 5×10^{-14} cm^3/s on the removal rate of OH($v = 9$) by Ar and He. A potentially more important relaxation partner is O_2, present as a <10% impurity to O_3. However, the known rate for OH($v = 9$) relaxation by O_2 ($k_{O_2} = 1.7(11) \times 10^{-11}$ cm^3/s [11]) is more than an order of magnitude smaller than by O_3 itself, which would translate into <1% contribution to the observed rates.

The major contributors to relaxation are ammonia and ozone, i.e., $k_{rise} \approx k_{NH_3}[NH_3] + k_{O_3}[O_3]$. To isolate individual rate constants k_{NH_3} and k_{O_3}, one can plot $k_{rise}/([O_3] + [NH_3])$ against the mole fraction of ammonia, $\chi_{NH_3} = [NH_3]/([O_3] + [NH_3])$, which yields k_{O_3} and k_{NH_3} in the limit of $\chi_{NH_3} = 0$ and 1, respectively (see Fig. 3). The data in Fig. 3 reflect more than 100 individual measurements at various NH_3 and O_3 densities and multiple He or Ar buffer-gas pressures, predominantly probing on the $v = 11 \leftarrow 9$ P_{1e} (3.5) OH transition. A least squares fit to the combined data set yields $k_{NH_3} = 7.60(50) \times 10^{-10}$ cm^3/s (intercept at $\chi_{NH_3} = 1$) and $k_{O_3} = 1.37(15) \times 10^{-10}$ cm^3/s (intercept at $\chi_{NH_3} = 0$), where numbers in parentheses represent 2σ uncertainties. This analysis is also confirmed by conventional one-component plots of rates vs. O_3 or NH_3 density, which yield statistically indistinguishable results from the two-component fits described above.

These are remarkably fast relaxation rates, equal to or greater than the gas-kinetic limit. Kinetic complications from impurities are therefore extremely unlikely but worth considering. For example, the excimer laser also photolyzes a

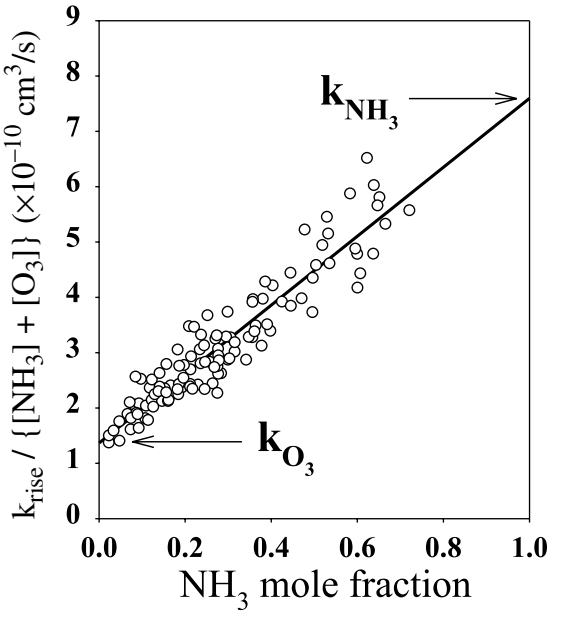

Fig. 3. Two-component analysis of the rise-time data. The intercepts at $\chi_{NH_3} = 0$ and $\chi_{NH_3} = 1$ yield the corresponding bimolecular removal rate constants (uncertainties in parentheses are 2σ): $k_{NH_3} = 7.60(50) \times 10^{-10}$ and $k_{O_3} = 1.37(15) \times 10^{-10}$ cm^3/s.

small fraction of O_3 molecules ($\sigma_{O_3}(193\text{ nm}) = 4.3 \times 10^{-19}$ cm^2 [12] vs. $\sigma_{NH_3} = 1.2 \times 10^{-17}$ cm^2 [13]) to produce $O(^1D)$ atoms, which can rapidly react with NH_3 to generate an alternate source of OH. However, this reaction can energetically populate only up to OH($v = 4$), which is not probed by the IR laser. Similarly, at the low UV photolysis intensities and short time-scales explored herein, radical–radical reactions such as

$$OH(v') + OH(v'') \rightarrow \text{products} \quad (7)$$

are completely negligible. Specifically, absolute OH radical concentrations can be measured directly from the integrated IR absorbances to be $[OH(v = 9, \text{ all } J)] \approx 1 \times 10^{11}$ cm^{-3}. This yields a conservative upper limit of 5×10^{12} cm^{-3} for *overall* OH density summed over all vibrational and rotational states, [4,5] which is $\approx 10^2$- to 10^3-fold lower than necessary to generate kinetic intereference even for gas-kinetic rates. Finally, these studies have been performed over at least an order of magnitude in OH densities (by photolysis intensity and O_3 concentration dependence); the consistency of the kinetic analysis results explicitly rule out nonlinear radical–radical processes under the present range of experimental conditions.

4. Discussion

The rate constants for removal of OH($v = 9$) by NH_3 and O_3 are extremely fast and warrant further discussion. The experimental removal rate of OH($v = 9$) by O_3 ($k_{O_3} = 1.37(15) \times 10^{-10}$ cm^3/s) is in relatively good agreement with the result of Greenblatt and Wiesenfeld [14], who inferred $k_{O_3} \approx 2 \times 10^{-10}$ cm^3/s from emission-based measurements (no error bars reported). This room temperature rate constant translates into an average reactive cross-section of $\sigma_{O_3} = k_{O_3}/\langle v_{rel} \rangle = 19 \pm 2$ Å^2, i.e., comparable to its ≈ 36 Å^2 collision cross-section (see Table 2) and implying that OH($v = 9$) is quenched with near gas-kinetic efficiency by O_3.

It is interesting to consider possible competition between relaxation and chemical reaction pathways. Teitelbaum et al. [15] was the first to suggest that OH($v = 9$) removal was dominated by vibrational relaxation and not by chemical reaction. This was largely based on the fact that the rate for vibrationally unexcited OH($v = 0$), where loss is purely by chemical reaction with O_3 to form $HO_2 + O_2$, is over 1500 times slower ($k = 8.4(8) \times 10^{-14}$ cm^3/s [16]). This would represent a rather significant enhancement in reactivity due to the vibrational excitation, despite the fact that the chemical pathway to form HO_2 and O_2 does not require OH bond extension in the transition-state region. From the simple A + BC Polanyi rules, for example, one would not anticipate strong promotion of the chemical reaction pathway with OH vibrational excitation.

On the other hand, new chemical channels can also be accessed at these higher energies [17], which provide a simple rationale for large vibrational enhancement effects. For example, bond breaking to form $H + O_2 + O_2$ or $OH + O_2 + O$ becomes energetically open for OH($v \geqslant 3$), which from Polanyi rules might be sensitive to OH vibrational excitation. One might argue that the

Table 2
Total removal rates of OH($v = 9$) by collision partners measured in this work and in [11][a]

Collider	Relaxation rate (cm^3/s)	Average cross-section ($Å^2$)	Hard-sphere cross-section ($Å^2$)	
NH_3[b]	$7.60(50) \times 10^{-10}$	89 ± 6	33[c]	39[d]
O_3[b]	$1.37(15) \times 10^{-10}$	19 ± 2	36[c]	–
N_2O[e]	$6.4(10) \times 10^{-11}$	9.0 ± 1.4	35[c]	40[d]
CO_2[e]	$5.7(9) \times 10^{-11}$	8.0 ± 1.3	35[c]	40[d]
O_2[e]	$1.7(11) \times 10^{-11}$	2.3 ± 1.5	32[c]	32[d]
Ar[b]	$<5 \times 10^{-14}$	<0.007	32[c]	32[d]

[a] The third column provides thermally averaged collision cross-sections, $\sigma_{O_3} = k_{O_3}/\langle v_{rel}\rangle$. The last two columns contain hard-sphere collision cross-sections estimated from viscosity and virial coefficients (for OH, the average of H_2O and HF effective diameters is used, $d_{OH} = 3.4$ Å).
[b] Present work.
[c] Estimated from cubic equation of state coefficients.
[d] Estimated from viscosity.
[e] Ref. [11].

increased OH($v = 9$) quenching cross-section with O_3 is the result of chemical reaction occurring *in parallel* with vibrational relaxation. This provides especially interesting comparison with extensive work by Price et al. [18] on quantum-state dependent vibrational self-relaxation of $O_2(v)$, where competition between vibrational relaxation and reaction leading to $O + O_3$ is implicated for $O_2(v \geqslant 26) + O_2$ collisions. By way of further empirical support, nonreactive quenchers such as CO_2 and N_2O [11] are much less efficient than O_3 in collisional removal of OH($v = 9$) (see Table 2). In any event, the present data suggest that competition between vibrational relaxation and chemical reaction dynamics of OH($v = 9$) with O_3 could be quite interesting and warrants further theoretical investigation.

A more dramatic result of this study is the removal of OH($v = 9$) by NH_3, for which the observed rate, $k_{NH_3} = 7.60(50) \times 10^{-10}$ cm^3/s, corresponds to a collision cross-section of 89(6) $Å^2$, i.e., larger than the hard-sphere limit (Table 2) by a two- to three-fold. With such fast rates, one is justifiably concerned with possible contamination by other relaxation processes. For example, reaction (2) produces OH with substantial *rotational* excitation [4]. Thus, the observed kinetics could in principle be complicated by rotational, spin–orbit, and lambda-doublet changing collisions into (or out of) the OH probe state. However, the time-dependent Boltzmann plots in Fig. 4 conclusively

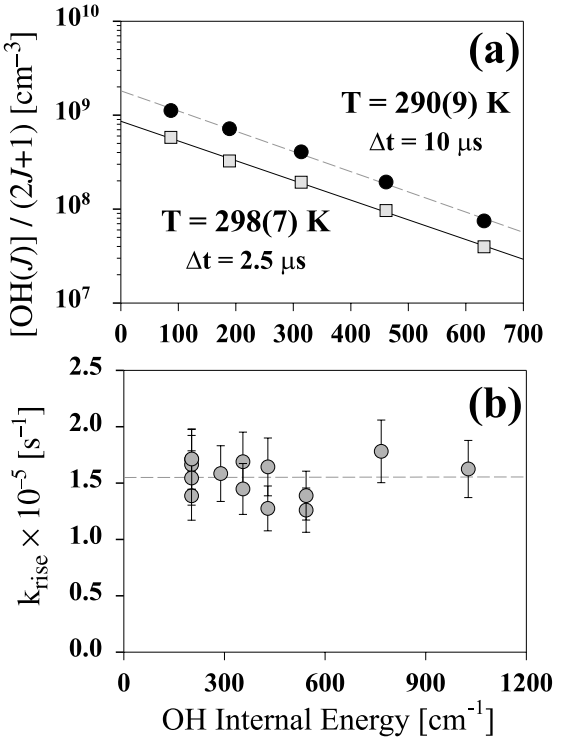

Fig. 4. Evidence for rapid rotational equilibration. (a) A Boltzmann plot of OH($v = 9$) at 2.5 μs and 10 μs after the photolysis laser pulse, both indicating room temperature rotational distributions. (b) Within experimental uncertainty, all *rise*-times (i.e., OH *removal* rates) are independent of OH internal energy. The horizontal axis represents different rotational ($J = 2.5$–7.5), spin–orbit ($^2\Pi_{1/2}$ and $^2\Pi_{3/2}$), and lambda-doublet [$\Pi(A'')$ and $\Pi(A')$] energy levels with respect to OH ($^2\Pi_{3/2}(A')$, $v = 9$, $J = 3/2$).

demonstrate that OH rotational equilibration to the cell temperature is quickly established (<2.5 μs) and remains constant after the excimer laser pulse. The bottom panel shows that measured rise-times are independent of the internal energy of the probed state. In fact, these results are not surprising given that the spin–orbit changing, spin–orbit conserving, and lambda-doublet changing collisions of OH with Ar and He (disregarding small propensities for the total parity conservation) all occur with comparably high probabilities [19,20].

We briefly consider the possible role of chemical acceleration of this quenching process. The exothermic H atom abstraction reaction of OH($v = 0$) from NH_3 is quite slow [21], and from simple A + BC models not anticipated to be strongly promoted by vibrational excitation of the OH 'spectator' bond. One important distinction with $OH + NH_3$ is the much stronger H–NH_2 vs. O–O_2 bond, which energetically closes off analogous chemical channels to form $O + H_2 + NH_2$, even up at OH($v = 9$) internal energies. Thus, if Polanyi rules provide the correct qualitative picture for polyatomic systems, this exceptionally fast OH($v = 9$) removal by NH_3 is not easily ascribed to chemical reaction, at least not via a direct atom abstraction mechanism. On the other hand, rapid long-range V–V transfer in the entrance channel from OH($v = 9$) to the NH stretching manifold in NH_3 could provide exactly the right excitation to successfully promote subsequent H atom transfer near the transition-state region. Indeed, V–V transfer rates are governed by the same physics as IR dipole transition intensities, and therefore would be expected to be especially swift for near resonant exchange between the strongly absorbing and emitting OH/NH stretch manifolds [22]. This is born out by experimental studies: NH_3 vibrational quenching of OH(v) is extremely rapid, with $k(v) = 0.25 \times 10^{-10}$, 1.0×10^{-10}, and 3.0×10^{-10} cm^3/s [23–25] for $v = 1$, 2 and 3, respectively. Interestingly, near resonant V–V transfer theory [22] between diatomics predicts these relaxation rates to scale *linearly* with vibrational quantum number, or in other words, $k(v)/v \approx$ constant. In fact, the data for OH($v = 1, 2, 3$) + NH_3 indicate a *growth* in $k(v)/v = 0.25$, 0.5, 1.0×10^{-10} cm^3/s, where the increase is presumably due to anharmonic lowering of the OH(v) level spacing ($\omega_e \approx 3737$, $\omega_e x_e \approx 84.8$ cm^{-1}) into resonance with the ≈300 cm^{-1} lower NH stretch manifold ($v_1 \approx 3337$ and $v_3 \approx 3444$ cm^{-1}) in NH_3 [26,27]. The role of such anharmonic detuning has been clearly demonstrated by extensive studies of resonant vibrational relaxation of O_2 [28]. This V–V resonance between OH(v) and NH_3 will 'detune' for $v > 5$, which would predict a decrease in $k(v)/v$ ratio by $v = 9$. Indeed, this is consistent with the experimental value of $k(v)/v = 0.85 \times 10^{-10}$ cm^3/s for OH($v = 9$), i.e., comparable to the ratios observed for $v \approx 1$–3, and lends further support to a long-range V–V energy transfer process.

As a final comment, near resonant V–V transfer between OH($v = 9$) and NH_3 would nominally require an 'overtone' (i.e., $\Delta v_{OH} = -2$, $\Delta v_{NH} = +1$) relaxation process, which for the corresponding emission event would be forbidden at the harmonic oscillator level. However, these simple selection rules are broken in OH by anomalously high curvature in the dipole moment function [29], which leads to a dramatic enhancement of overtone transition strengths at these high v levels. For example, the $v = 9 \rightarrow 7$ overtone emission strength of OH is more than an order of magnitude stronger than the corresponding $v = 9 \rightarrow 8$ fundamental emission. Indeed, a similar enhancement effect occurs in absorption and makes the present studies feasible in spite of probing on an overtone $v = 11 \leftarrow 9$ band. This discussion raises interesting questions about the nature of V–V transfer in systems such as OH with high mechanical and electrical anharmonicity, which would represent interesting directions for further experimental and theoretical exploration.

Acknowledgements

Financial support by the Air Force Office of Scientific Research is gratefully acknowledged. W.W.H. thanks the National Research Council for a postdoctoral fellowship.

References

[1] Y.L. Yung, W.B. DeMore, Photochemistry of Planetary Atmospheres, Oxford University Press, New York, 1999.
[2] W.R. Pendleton Jr., P.J. Espy, M.R. Hammond, J. Geophys. Res. 98 (1993) 11567.
[3] J.A. Dodd, S.J. Lipson, J.R. Lowell, P.S. Armstrong, W.A.M. Blumberg, R.M. Nadile, S.M. Adler-Golden, W.J. Marinelli, K.W. Holtzclaw, B.D. Green, J. Geophys. Res. 99 (1994) 3559.
[4] P.E. Charters, R.G. Macdonald, J.C. Polanyi, Appl. Opt. 10 (1971) 1747.
[5] H. Ohoyama, T. Kasai, Y. Yoshimura, H. Kimura, K. Kuwata, Chem. Phys. Lett. 118 (1985) 263.
[6] D.D. Nelson, A. Schiffman, K.R. Lykke, D.J. Nesbitt, Chem. Phys. Lett. 153 (1988) 105.
[7] R.A. Copeland, B.R. Chalamala, J.A. Coxon, J. Mol. Spectrosc. 161 (1993) 243.
[8] A. Goldman, W.G. Schoenfeld, D. Goorvitch, C. Chackerian Jr., H. Dothe, F. Melen, M.C. Abrams, J.E.A. Selby, J. Quant. Spectrosc. Radiat. Transfer 59 (1998) 453.
[9] K. Mauersberger, D. Hanson, J. Barnes, J. Morton, J. Geophys. Res. 92 (1987) 8480.
[10] W.B. DeMore, S.P. Sander, D.M. Golden, R.F. Hampson, M.J. Kurylo, C.J. Howard, A.R. Ravishankara, C.E. Kolb, M.J. Molina, Chemical Kinetics and Photochemical Data for Use in Stratospheric Modeling: Evaluation Number 12, JPL, Pasedena, 1997.
[11] B.R. Chalamala, R.A. Copeland, J. Chem. Phys. 99 (1993) 5807.
[12] L.T. Molina, M.J. Molina, J. Geophys. Res. 91 (1986) 14501.
[13] M. Suto, L.C. Lee, J. Chem. Phys. 78 (1983) 4515.
[14] G.D. Greenblatt, J.R. Wiesenfeld, J. Geophys. Res. 87 (1982) 11145.
[15] H. Teitelbaum, P. Aker, J.J. Sloan, Chem. Phys. 119 (1987) 79.
[16] A. Kulcke, B. Blackmon, W.B. Chapman, I.K. Kim, D.J. Nesbitt, J. Phys. Chem. A 102 (1998) 1965.
[17] T.G. Slanger, D.L. Huestis, Int. J. Chem. Kinet. 17 (1985) 713.
[18] J.M. Price, J.A. Mack, C.A. Rogaski, A.M. Wodtke, Chem. Phys. 175 (1993) 83.
[19] K. Schreel, J. Schleipen, A. Eppink, J.J. ter Meulen, J. Chem. Phys. 99 (1993) 8713.
[20] I.J. Wysong, J.B. Jeffries, D.R. Crosley, J. Chem. Phys. 94 (1991) 7547.
[21] N. Fujii, H. Miyama, T. Asaba, Chem. Phys. Lett. 80 (1981) 355.
[22] J.T. Yardley, Introduction to Molecular Energy Transfer, Academic Press, New York, 1980.
[23] K.J. Rensberger, J.B. Jeffries, D.R. Crosley, J. Chem. Phys. 90 (1989) 2174.
[24] G.A. Raiche, J.B. Jeffries, K.J. Rensberger, D.R. Crosley, J. Chem. Phys. 92 (1990) 7258.
[25] S.G. Cheskis, A.A. Iogansen, P.V. Kulakov, O.M. Sarkisov, A.A. Titov, Chem. Phys. Lett. 143 (1988) 348.
[26] T. Shimanouchi, Tables of Molecular Vibrational Frequencies, NSRDS-NBS 39 (1972).
[27] K.P. Huber, G. Herzberg, Constants of Diatomic Molecules, Van Nostrand Reinhold, New York, 1979.
[28] J.A. Mack, K. Mikulecky, A.M. Wodtke, J. Chem. Phys. 105 (1996) 4105.
[29] D.D. Nelson Jr., A. Schiffman, D.J. Nesbitt, J.J. Orlando, J.B. Burkholder, J. Chem. Phys. 93 (1990) 7003.